

ENHANCED SEAT BELT MODELLING PROCESS TO IMPROVE PREDICTIVE ACCURACY OF DUMMY RESPONSES IN FRONTAL IMPACT

Tom Voigt

Werner Schrenk

Harald Zellmer

Autoliv B.V. & Co. KG, Elmshorn, Germany

Paper Number 11-0151

ABSTRACT

Computer simulations are a standard tool for improving vehicle safety. In these simulations, predictions about dummy responses and injury assessment values can be made. For accurate predictions, the behaviour of the retractor as a major part of the seatbelt system has to be known. Tests are needed to generate this knowledge and incorporate it into a simulation model. Standard sled tests are too expensive and generally have too much deviation to be a useful correlation environment. Component tests are of limited use due to the lack of interaction, or the coupling between the different crash phases. Subcomponent tests are only useful if a robust simulation model already exists. Furthermore, a model structure is needed which reflects all main effects of the retractor in a time independent way.

Thus, there are two needs for an enhanced modelling process: A correlation test device as well as a model concept which reflects the interaction in a simple and robust way.

This paper demonstrates a new process on how a retractor model can be correlated in different solvers with a component test, within the typical working points of a retractor. The improved process is based on a new easy test assembly for retractors (ETAR) and on a general model structure (GMS) for the retractor models. The new component test assembly reflects the three phases of pretensioning, coupling and load limiting of a frontal crash without the need of a sled and/or dummy. Furthermore, for the correlation of retractor models in different solver codes, ETAR allows to generate test data in a fast and simple way with low deviation. The GMS implements all the main functionalities of a retractor and due to the GMS, the tuning of the models is easily transformed into other solver codes, commonly used for crash simulations.

Correlations between test and simulation for different load-cases and different retractors in

different solvers demonstrates the applicability of ETAR and GMS for an improved retractor modelling.

INTRODUCTION

A good and reliable crash performance in frontal impact tests, for both homologation and for consumer ratings, is a major prerequisite in car design. During the process of system layout for frontal impact, all parts of the restraint system have to be adapted to the particular vehicle environment. This is done by physical crash tests and by computer simulations simultaneously. In the early phase of the development, the tests are performed to verify the simulated results, and the simulation models are used to optimize the parameters. Thus, simulation models of the restraint system must be available and reliable.

The seat belt is a fundamental part of the occupant restraint system. Modern seat belts have a pyrotechnical pretensioner unit to reduce belt slack and tighten the occupant to the car in the first milliseconds of a crash. The pretensioner device can act at the retractor, at the buckle, or at the anchor plate. Combinations of two pretensioners are possible. In the phase of maximum occupant loading, after about 50 ms, a load limiter keeps the belt force at a constant level, which is - depending on the specific car and seating position - between 3 kN and 6 kN.

Crash tests do not need to be performed in a real physical environment. Crash tests can be done by physical crash tests and by computer simulations. The physical tests are time-consuming and the information is limited to the amount and kind of sensors. Computer simulations are an important tool to overcome these deficits. In such simulations, numerical models calculate the behaviour of the dummy during the frontal crash. This kind of simulation is also called system simulation or occupant protection simulation. Injury assessment values as well as forces in the restraint system are generated by such models. For system simulation

models, the predictability of the whole system depends on the accuracy of every subcomponent. Without a validated retractor model, a predictive crash occupant protection simulation model will not be possible.

Ideally, these system simulation models should be predictive for different load cases. However, different load cases will in turn change the working point of the retractor. Consequently, the retractor model is required to be predictive for different working points. If a model is predictive for different load cases, the model will be called robust.

So, the predictive accuracy of dummy responses in such system simulations depends not only on the accuracy of the dummy model, but also on the accuracy of the interaction of components. This generates the apparent need for a robust retractor simulation model that has to be validated for different working points. In turn, tests with different working points are needed to correlate the retractor model.

The retractor itself is a component with different functional subcomponents. These are in interaction with other subcomponents and components outside of the retractor. In general, these subcomponents cannot be validated separately for a robust retractor model, due to the nonlinear interaction in the system.

The different vehicle manufacturers use different numerical solver codes in their vehicle development processes. The chosen solver has an influence on how different effects can be implemented into the model. Thus, the solver has an influence on the model structure and due to this, also on the approach and the effort associated with the correlation.

For correlations with different working points, different model structures for different solvers are needed for predictive component models.

The more effects and more load cases which should be reflected by a model will raise the amount of needed tests for the correlation. To validate retractor models, tests in a simplified environment are performed. Classically, a sled test according to ECE-R 16 /1/ using a Hybrid III 50th-percentile dummy /2/ is performed, a corresponding simulation model is set up and parameters such as belt forces, webbing pay-in by pretensioning and pay-out by load limiting are adjusted. The main drawback is that the validation has to be done separately for each solver, especially as each solver has its own dummy models.

The usage of frontal crash simulation to improve the predictive accuracy of dummy response is limited by the performance of the simulation models of the subcomponents (e.g. retractor). Thus, to generate a robust and reliable retractor model, in the classical correlation manner, a substantially high correlation effort is required. This paper presents a process showing how robust and reliable models can be

correlated, in different solvers, in a fast and effective manner.

CORRELATION PROCESS

Figure 1 shows the new fundamental correlation process. The process for the validation is the same for all solvers. Furthermore, the functionalities of the test rig as well as for the component model should be the same for all solvers. This is of fundamental importance to minimize the effort for correlating the same models in different solver codes. The model is correlated for different load cases (LC) in an easy test assembly (ETA) model environment.

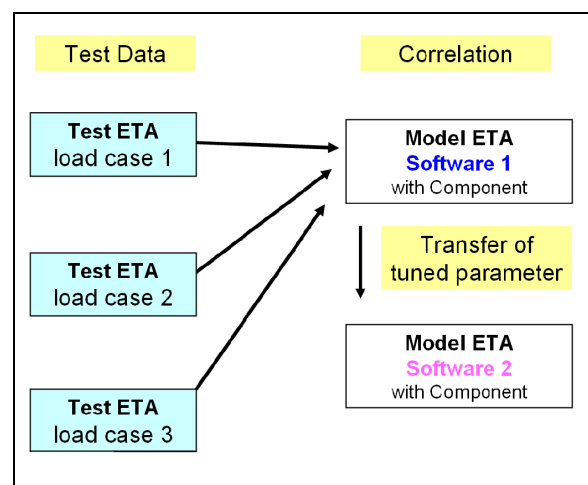


Figure 1. Principle correlation process for different solver.

Once a correlation in one solver code is done, the tuned characteristics of one model can be used for the same model in the other solver codes. Due to small solver related differences in the subroutines as well as the available sensors and functions in the different codes, the simulation results are bound not to be exactly the same. However, if all physical parameters are the same, the results of the different solvers should correlate well to each other.

There are two principle ways how a component model can be generated. The first is a black box model in which the behaviour of the subcomponents are not reflected. For such a model of a retractor, only the force and belt pull out (pull in) behaviour at the retractor have to be correlated for the different load cases. In an effect based model, the functional subcomponents are reflected. This model is also called white box model, in which the origin of the component behaviour is allowed to be analysed. Due to the interaction in a system, every subcomponent of

such a model has to be validated for different load cases. In general, the model structure of a white box model is more complex than that of a black box model, but a white box model can also be used for gaining an understanding of effects and subcomponent analysis. Due to this, a white box structure is chosen. An additional benefit of this kind of structure is the possibility to use the already available subcomponent characteristics.

ETAR

Numerous tests exist for the validation of retractors and their functionalities. These tests are made for a subcomponent of the retractor or for the restraint system. The subcomponent tests are not useful because they do not reflect the interaction of the individual subcomponents with each other. The restraint system tests have their focus on the whole restraint system and do not concentrate on the component. In general the restraint test rigs have more data variation and are more time-consuming. In the following, we will describe the development of a fast and repeatable component test method which can substitute a sled test for retractor validation and of which a CAE model can easily be build up in each solver /3/.

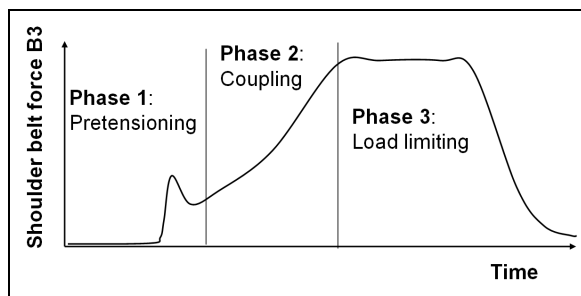


Figure 2. Schematic illustration of the 3 phases of a sled test.

The requirements to a correlation test for retractor models that are to be implemented in system simulation model are different to those tests, which are designed for evaluating injury assessment values. For example, although the easy test assembly for retractors (ETAR) has to reflect all important crash phases of the retractor (Figure 2), thus maintain resemblance to the actual working points of the retractor model, the assembly should also have low variation, should not be time-consuming, should have only a few parameters and should be able to be modelled in all relevant solvers in a simple manner. The geometry of the test rig can be much simpler than the geometry of a belt restraint system.

However, it is essential that the working points of the retractor in such an easy test assembly must be in the same range as in real crashes test environments.

In order to fit these requirements, ETAR was built in two steps. In the first step, the requirements to the pretensioner performance were defined, and in a second step the coupling and load limiting phases were added.

It is assumed that a system with a damping function, a dynamic mass and an elasticity (two linear springs) can lead to an environment with a realistic retractor working point for the pretensioning, see Figure 3. This subcomponent of ETAR is called ETAR1. The fundamental initial parameters are shown in Figure 3b.

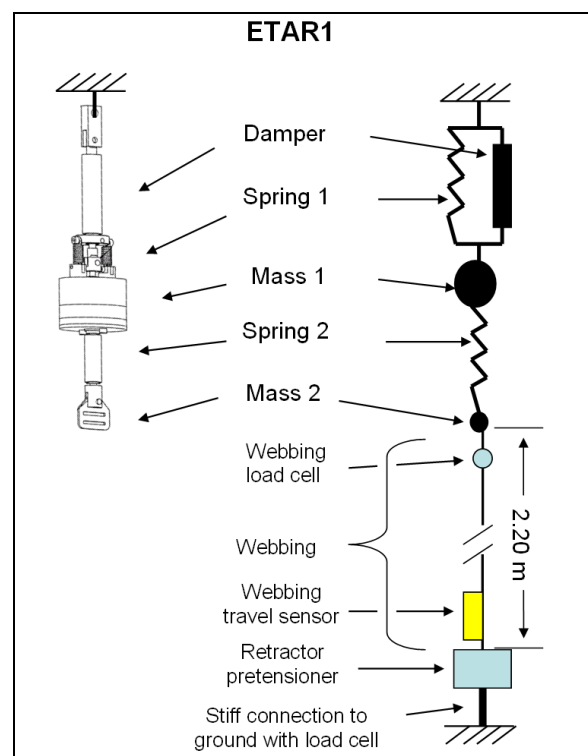


Figure 3. Basic hardware ETAR set up for pretensioning phase.

ETAR1 is vertically orientated at the top of ETAR and connected to the retractor pretensioner by 2.20 m of webbing, as shown in Figure 4a. A force measurement is provided at the retractor fixation point in addition to a webbing load cell at the ETAR1 end of the webbing. A start set of masses, spring and damper characteristics was obtained by simulation.

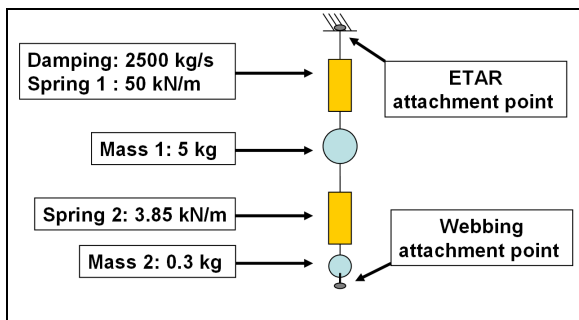


Figure 3b. Parameter for the basic ETAR set up for pretensioning phase.

In order to cover a wider area around the working point of the retractor, two additional load cases were introduced. These different working points should reflect the adaptive behaviour of the retractor for different preloads. The first is a “slack” load case, representing car environments with yielding parts, such as seat belt buckle fixation, webbing being routed over seat cushions, etc. In these environments, more pretensioning distance is achieved. It is known from pre-tests that a very low preload (below 20 N) yields in less repeatability. For this reason, a low preload of around 50 N has to be applied, therefore Spring 2 must be substituted by a softer one. The second additional load case is performed with a high preload (~ 400 N), which accounts for load cases with a late firing of the pretensioner, when the dummy's forward displacement is already loading the belt system. Again Spring 2 has to be replaced, this time by a stiffer one.

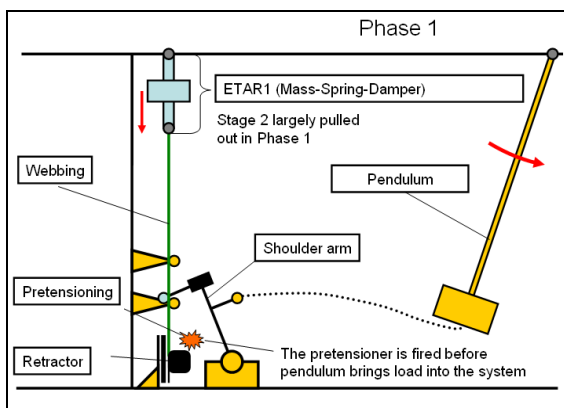


Figure 4a. ETAR set up for webbing pull in while pretensioning. No influence of shoulder arm on pretensioning.

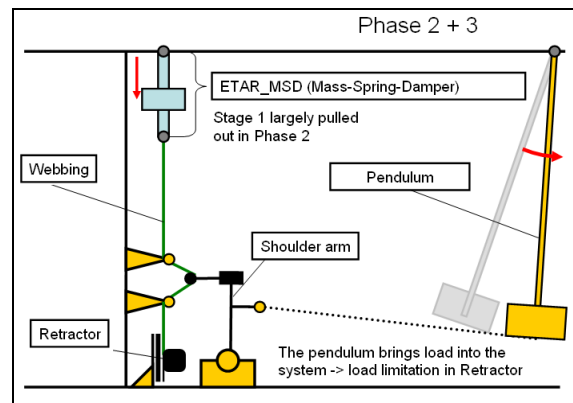


Figure 4b. ETAR set up for webbing pull out after pretensioning.

In a second step, a device to emulate phases 2 & 3 (ETAR2) is added. It is set up in such a way that the events in phase 1 is not disturbed by it. A shoulder arm, accelerated via a string by a pendulum is pulling out webbing between ETAR1 and the retractor. Due to the geometry of ETAR2 the pull out velocity is similar to that in a sled test as opposed to that in a direct pull of the pendulum.

A high repeatability compared with common system test like AK static or ECE R16 sled tests /1/ can be achieved, caused by only a few parameters in the comparatively simple geometry.

In Figure 5, the force at the retractor for 3 identical tests are shown. The force and the pull in starts before 0 ms because the data acquisition was triggered by the pendulum, which will trigger before 0 ms. In the beginning at 2 ms and 10 ms two distinct pretensioner peaks can be identified.

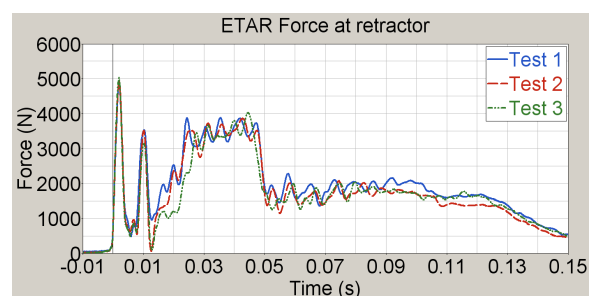


Figure 5. Retractor force test data versus time; three ETAR test repetitions.

After the pretensioning, the force rises up to the first load limiter level. This coupling phase will be due to the impact of the shoulder arm in the belt system (Figure 4b). At 25 ms the load limiter is limiting the force on a level of 3500 N. The force drops down at 45 ms is due to a switching load

limiter which is switched to a second, lower load limiter level.

In Figure 6 the belt pull outs at the retractor for the same 3 identical tests as in Figure 5 are shown. In the beginning a belt pull in (negative belt pull out) up to 150 mm is reached. Thereafter, during the coupling phase of ETAR, the constant level of belt pull out is reached. The belt pull out for the load limiting starts at 25 ms and stops at 95 ms. During load limiting, more than 500 mm webbing is pulled out of the retractor.

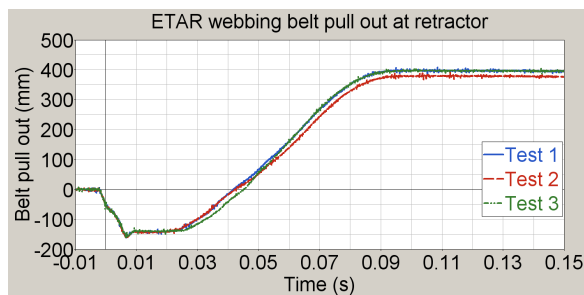


Figure 6. Retractor webbing pull out test data versus time; three ETAR test repetitions.

These tests show the capability of ETAR to detect the force and belt pull out of the retractor for all three phases of a crash.

GENERAL MODEL STRUCTURE

This chapter presents an overview over the general model structure (GMS) of the retractor model and the working principles of the GMS. The GMS retractor simulation model is implemented in several solver codes, such as Madymo, LS-Dyna, PAM-Crash, Abaqus. Although the model structure and characteristics are implemented in an identical manner in all solvers, not all functionalities, settings and switching systems can be implemented in an identical manner. This is due to the varying capabilities of the different solver codes.

The retractor simulation model consists of twelve sequentially arranged translational joints. This GMS is invariant for all retractor simulation models and is referred to as the “chain-of-joints” (Figure 8). Each joint respectively represents some single, designated functionality of a physical retractor component (i.e. pretensioner, torsion bar, shear pins, etc.), or some characteristic effect (film spool, locking, etc.), or (pre-) loading conditions of a retractor. Each joint is modelled as a spring-damper sub-system.

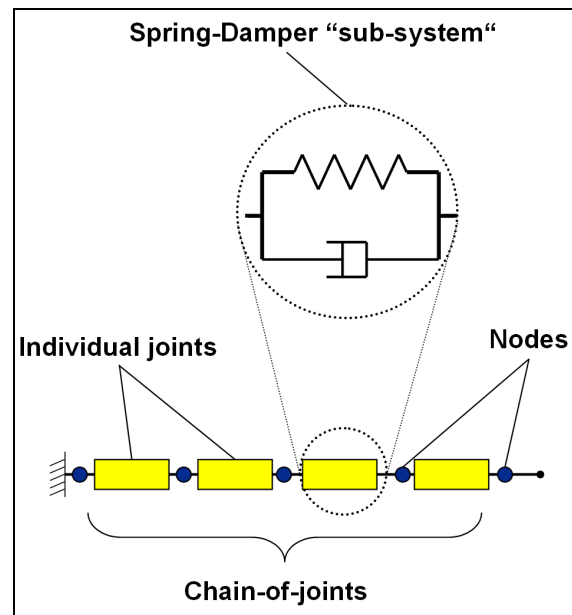


Figure 7. General model structure (GMS).

For the individual solvers, the joint types and material types are specifically selected in order to model the appropriate behaviour. Thereby, designated loading / unloading characteristics, hysteresis models and damping behaviours are specified for each joint. These functionalities are reserved for all joints but not necessarily always implemented. Finite lumped masses are implemented on the node between any two adjacent joints.

Generally, the one end of the chain-of-joints is to be attached to the vehicle, the other end to the webbing. This defined structure and sequence of the joints in the chain-of-joints is invariant.

All of the joints are always implemented for all retractor models. Not all joints are always active at any given point in time and/or are used in all retractor models. The deactivated joints are set as rigid. With regard to the FE-solver codes (LS-Dyna, PAM-Crash, Abaqus), it has to be noted that the joints are set as “rigid” by assigning a significantly high, yet finite, spring stiffness function to the spring component of the joint. Strictly speaking, such joints do have some remainder of elasticity, which however is considered insignificantly small such that these joints may essentially be considered to be “rigid”. Table 1 gives an overview of the individual functionalities and effects that are reserved for the individual joints.

Any specific retractor functionality is implemented into the corresponding retractor joint in the model in terms of characteristic spring stiffness function, damping function and a lumped mass. These parameters / characteristics may be given as scalars, linear or non-linear functions and vary depending on

the retractor model and the individual functionalities. The spring stiffness characteristics are generally given as linear / non-linear functions with hysteresis. The reserve joints can be used for necessary system tuning. This can be useful if additional elasticity form the attachment point in the vehicle or of the webbing or additional masses in the belt system, like load cells, should be reflected.

Joint	Function / Characteristic
Bolt	Retractor position in vehicle no characteristic
Frame	Deformation characteristics of frame
Spring	Preload conditions, retraction spring and pre-pretensioner
Stroke	Pretensioning of retractor
Locking	Locking travel of the lock dog Remainder of pressure in pipe
Shearpin	Shearing off of the shear pins
Load Limiter 1 (LL 1)	First stage of the load limiting
Load Limiter 2 (LL 2)	Second stage of the load limiting
Spindle	Inertial effects of the spindle
Filmspool	Film-spool effect
Reserve 1	Reserved joint for future use
Reserve 2	Reserved joint for future use May be used for system tuning

Table 1. Overview of functionalities and effects of the different joints of the chain-of-joints.

In order to model physical retractor behaviour, a switching system is implemented which activates / deactivates certain joints. Thereby the various retractor functionalities are activated / deactivated, as required. Various sensors are implemented reacting to displacements, velocities, accelerations, forces as well as user defined times to fire. Depending on the load case dynamics and the physical type of retractor that is being modelled, the various implemented sensors may or may not be triggered during the sequence of events, i.e. not all sensors must be triggered for a retractor to function normally. Time dependent switches are implemented as a back-up trigger. This can be used in the case the usual sensors are not available in the used solver version, the usual sensing of the switching fails, or to specifically end some functionality at some user defined time.

Apart from pretensioning and a constant load limiter, a non-constant load limiter can also be a

functional component of a retractor. The non-constant load limiting can be achieved by switching from a first load limiter level to a second load limiter level. This function is called Load Limiter Adaptive (LLA).

With predefined outputs of the joint displacement the functionality of the model can be easily controlled. In Figure 8, an example of the displacement of the individual joints of the chain is shown. A pre-simulation is used to implement a defined preload into the system. The retractor is able to pull in webbing (Stroke) and switch the load limiter level.

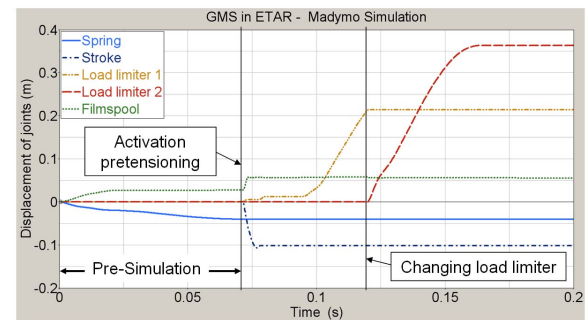


Figure 8. Example of joint displacement of the GMS in ETAR with pretensioning and adaptive load limiting (LLA).

In the pre-simulation, elasticity of the film-spool will be eliminated. Using a user defined time, the spring joint is locked by a time sensor, whereby the pre-simulation is ended. During subsequent pretensioning, the corresponding pretensioner joint will cause the specific elongation of the first load limiter joint as well as the film-spool joint, by which the elasticity of the film-spool is eliminated. The LLA is fired by a time sensor whereby the second load limiter joint is activated, which becomes the load carrying / dissipating path since the second load limiter has a lower load level than the first.

Using such a 1-D white box model, a GMS for all typical retractor types is available. In the next step the correlation results for the GMS in ETAR will be shown.

CORRELATION RESULTS

The correlation of the general structure can be done in different solvers. The starting tuning configuration is given by component tests and physical component parameters. Model parameters which are not known are the main tuning parameters. The main objective is to obtain a robustly correlated simulation model of the retractor component. Beside the damping, masses

and spring loadings, the hysteresis is important for the energy absorption and for the damping of oscillations.

In Figures 9a and 9b, a retractor without pretensining and with a constant load limiter is correlated in Madymo. Two different configurations are shown. The difference is the remaining webbing (RW) on the spindle. The RW is the webbing which is wound on the spindle and has an influence on the force levels and belt pull out behaviour of a retractor.

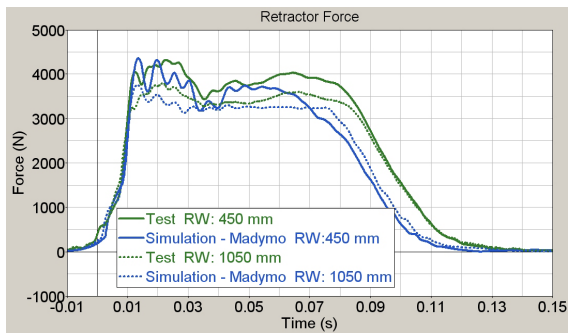


Figure 9a. Force versus time ETAR correlation plot of a retractor with two different remaining webbing (RW) on spindle.

Test and simulated forces of ETAR are shown in Figure 9a. The force level of the retractor with a RW of 450 mm is higher in test, as well as in simulation, than that for the retractor with a RW of 1050 mm, as it could be expected. The coupling phase is identical. In Figure 9b, test and simulated belt pull outs are shown. The belt output of the retractor with a RW of 450 mm is lower in test, as well as in simulation, than that for the retractor with a RW of 1050 mm.

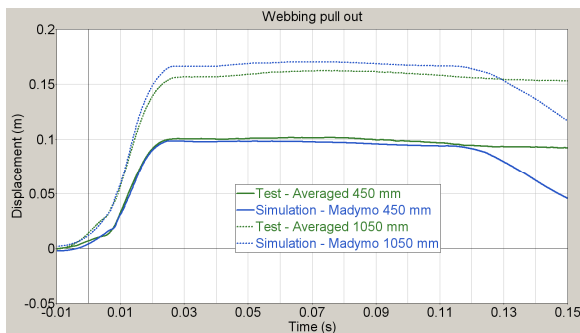


Figure 9b. Webbing pull out versus time ETAR correlation plot of a retractor with two different remaining webbing (RW) on spindle.

Figures 10a and 10b show a retractor with pretensining and with an adaptive load limiter, as

correlated in LS-Dyna. Two different preload conditions are shown.

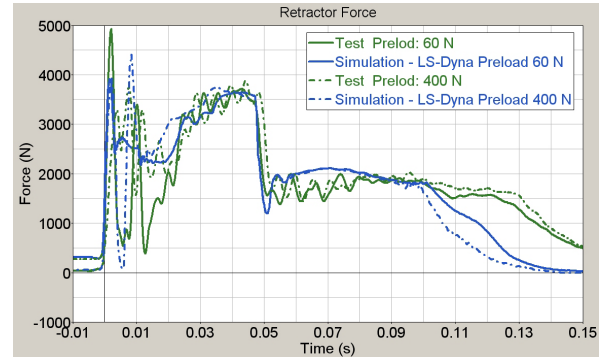


Figure 10a. Force versus time ETAR correlation plot of a retractor with two different preloads. Retractor with pretensining and adaptive load limiter (LLA).

Figure 10a shows the test and simulated retractor forces in ETAR. The force level in the coupling phase of the retractor with a preload of 60 N is lower in test, as well as in simulation, than that for the test with a preload of 400 N. The force levels during load limiting are identical. The earlier reduction of force levels from 100 ms onwards can be explained by the hysteresis function.

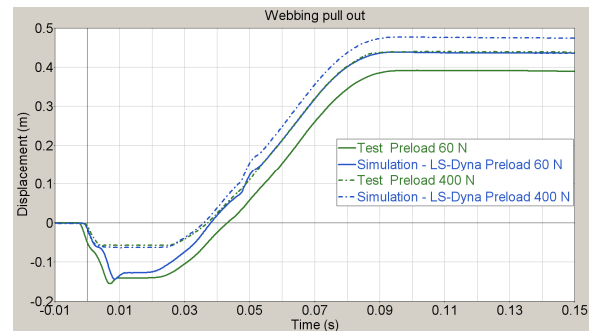


Figure 10b. Webbing pull out versus time ETAR correlation plot of a retractor with two different preloads. Retractor with pretensining and adaptive load limiter (LLA).

Figure 12 shows test and simulated belt pull out. The pull in of webbing during pretensining is higher in the lower preload LC. The load limiting starts earlier in the higher preload LC.

The Figures 11a and 11b show the simulation results of a retractor with pretensining and with an adaptive load limiter for different solver codes with a

150 N preload in ETAR. Modifications in the switching, as described previously, have to be done. The force levels as well as belt pull out signals a significantly comparable. The model structure is also the same for all models in all solver codes.

The observed differences are caused by differences in the subroutines as well as the available sensors and functions in the different solver codes. Thus, the simulation results are bound not to be exactly the same. These differences between the different solver codes are subject to further evaluations /4/.

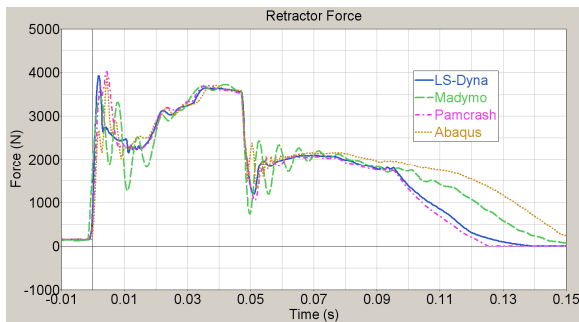


Figure 11a. Comparison of force versus time simulation results of different solvers.

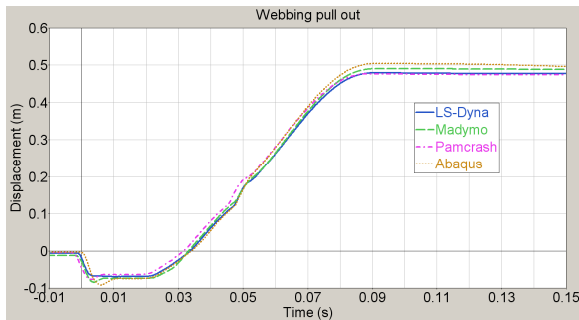


Figure 11b. Comparison of force versus time simulation results of different solver codes.

The correlation results of the different retractors in different preload configurations and in different solvers show the capability of the new validation procedure.

SUMMARY

An enhanced seat belt modelling process which can be used to improve the predictive accuracy the subcomponent model using an easy test assembly for Retractors (ETAR) in combination with a general model structure (GMS) for the retractor simulation models has been discussed.

Correlation test data for all frontal crash phases, relevant for occupant protection, can be generated

using ETAR. Furthermore, ETAR can be modelled nearly identically in the standard crash solver codes. With this test and simulation environment, a robust correlation can be done and the correlated functions of the general model structure (GMS) are exchangeable between different solver codes.

Correlation results between test and simulation for different load cases and different retractors models in different solver codes demonstrates the applicability of ETAR and GMS for an improved retractor modelling approach.

REFERENCES

/1/ ECE Regulation No. 16-06: Uniform Provision Concerning the Approval of: I. Safety belts, Restraint Systems, (...) II. Vehicles Equipped with Safety Belts, (...) <http://www.unece.org/trans/main/wp29/wp29regs/r016r6e.pdf>

/2/ National Highway Traffic Safety Administration (49 CFR PART 572) Anthropomorphic Test Devices, Subpart B.

/3/ Zellmer et al., Easy Test Assembly for Retractor Model Correlation; to be published

/4/ Voigt et al., to be published

Heavy Truck Occupant Restraint System - New approved Concepts and Development Methods

Frank Wollny
André Buchholz

Takata-Petri AG
R&D Centre Berlin

Germany

Paper Number 11-0354

Abstract

The efficiency of current frontal restraint systems in heavy trucks is not comparable to systems in passenger cars. There are no rating tests and legal requirements for the functionality of such systems. Therefore it is comprehensible that even non severe truck crashes in the field lead to non fatal but severe injuries with high rehabilitation costs. Another reason for the low efficiency of the current systems is the non-availability of an adequate development method.

During the development phase of a restraint system it is not possible to observe significant loads applied to the lower extremities by using the conventional test methods. However, the lower extremities gain more and more importance with respect to real world crash data. For that reason a new and approved test method will be introduced and published for the first time. It takes the intrusion of the cabin and interior displacement into account resulting in a good correlation between full scale tests and sled tests.

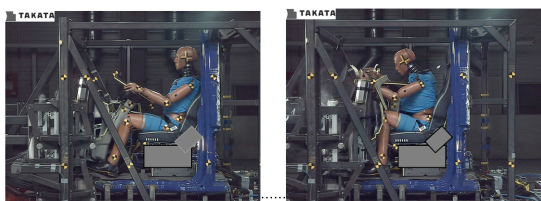


Figure 1: Takata-Petri Berlin Intrusion Device

The new method allows the verification of advanced and additional restraint system components such as optimized knee impact zones, knee airbags and activated steering column kinematics. A restraint system as described above provides optimized occupant kinematics with the effect of reduced loads.

The developed methodology is based on the so called "Trailer Back Barrier" test configuration. However, to date this configuration is not yet being used as a standard evaluation in the industry. This study is concentrating on cab over trucks due to the higher injury risk for the lower extremities compared to bonnet trucks.

Introduction

Occupant safety for passenger cars is on a very high level. Almost every new car generation has new features e. g. adaptive airbag modules to address the new customer rating requirements. The occupant size will be detected and the restraint system performance will be adjusted to the different driver or passenger weight. Up to 8 airbags within a passenger car is state of the art today.

For heavy trucks even driver airbags are only an optional feature presently.

Investigations of heavy truck accidents show that the lower extremities are heavily injured in almost every crash. Driver's pain and high rehabilitation costs occur, even at accidents with low relative velocity.

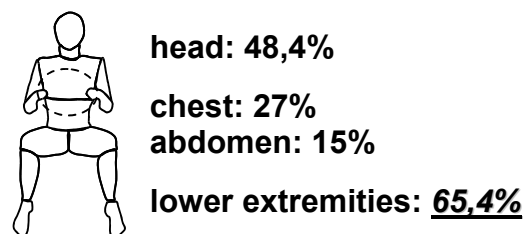


Figure 2: heavy truck occupant injuries based on 78 accidents [1]

Takata-Petri is aware of this issue and developed a test device especially to investigate heavy truck crashes in order to improve the restraint system for these special cars. In the end of this project, Takata-Petri was able to get an occupant safety level which is comparable to present passenger cars. The test device, called "intrusion device" is now a standard /patented/ development tool which shows the heavy truck crash behaviour in a way which was not able to show with usual test equipment. This test device and the results of the improvement of the heavy truck restraint system will be represented in this paper.

Heavy Truck Intrusion Device

Due to non existing regulations, the OEMs set their own crash scenarios based on internal accident data. Two kinds of impacts are used in heavy truck developments.

- Flat Wall Impact
- Trailer Back Barrier Impact (deformable barrier)

The crash velocity depends on the OEM philosophy.

During the trailer back barrier impact test, which simulates the impact at the end of a traffic jam, high cabin intrusion due to the height of the barrier /trailer/ occurs.



Figure 3: Trailer back barrier impact [2]

With standard test equipment it is not possible to reproduce the injuries e. g. high femur forces. Standard test sleds, which are used in passenger car developments, are usually stiff. This must be changed for heavy trucks. The cabin intrusion has to be taken into account.

Test Rig

The instrument panel is attached to a pendulum device, which allows displacement of the instrument panel. The kinematics of the pendulum can be adjusted to every trajectory of the real car instrument panel. This trajectory is taken from full scale crashes or numerical simulation. Due to two different deceleration devices the crash pulse of the instrument panel and the car body can be adjusted separately.

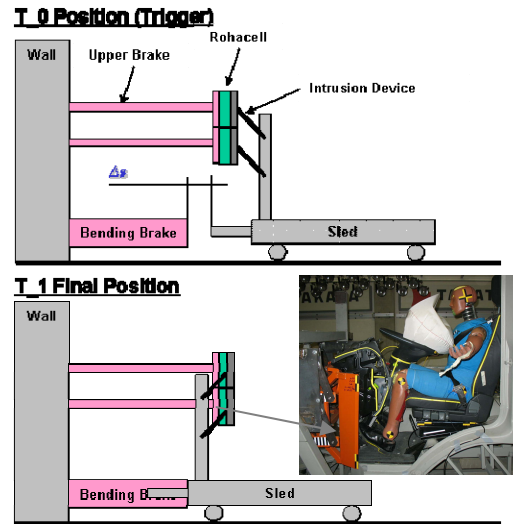


Figure 4: Function of Takata-Petri Intrusion Device

Heavy Truck Restraint System Optimization (HeRO)

Takata-Petri did an extensive pre-development project called HeRO, where the following restraint system components were considered by using the intrusion device.

- driver airbag
- knee airbag (KAB)
- energy absorbing knee bolster
- active steering column (ASC)
- belt pre-tensioner
- belt load limiter

By using these restraint system components a step by step improvement can be seen up to the already mentioned level of modern passenger cars.

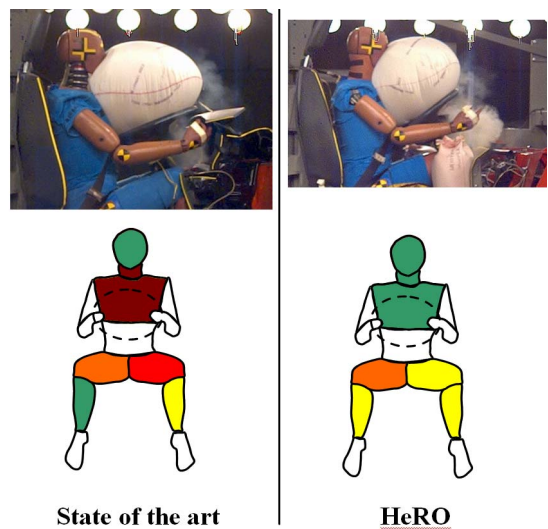


Figure 5: Comparison of restraint system performance between “state of the art” and “HeRO” based on Euro-NCAP assessment

Knee Impact Zone

The instrument panel intrusion device enables us to optimize the knee impact zone by using sled tests because for the first time it was possible to observe similar load characteristics of lower extremities in sled tests and full scale tests.

The first attempt was to design the knee impact zone with energy absorbing deformable structures. The effect could be clearly observed in the sled test results:

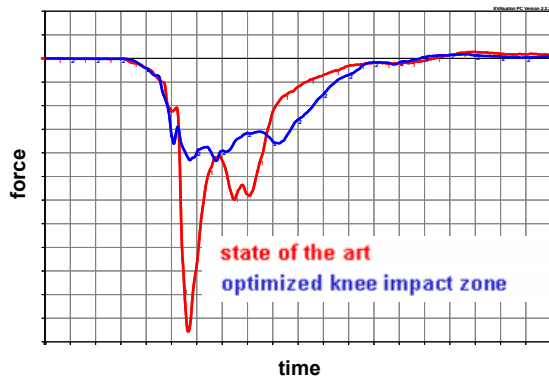


Figure 6: Femur loads with and without deformable structures

Even if the femur force could be reduced significantly, there is still an unfavourable occupant kinematics. And even worse: due to less pelvis restraint a more severe chest – steering wheel contact occurs.

Knee Airbag (KAB)

To improve the occupant kinematics the knee airbag is a well known feature. An early force application to the knees is expected. At the same time the load characteristics is biomechanically more sufficient.

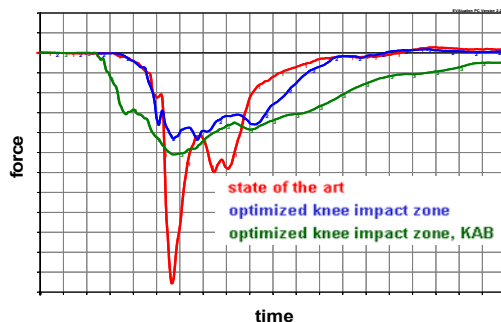


Figure 7: Impact of knee airbag on femur loads



Figure 8: Impact of knee air bag on dummy kinematics

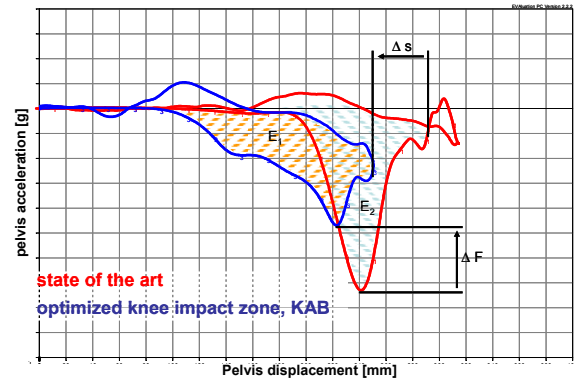


Figure 9: different way of energy absorption shown by pelvis acceleration vs. pelvis displacement

Because of the protruding steering column in the knee impact area, two single knee airbags, one for each knee have to be installed (dual knee airbag).



Figure 10: Application of two knee airbags for the driver (dual knee airbag)

Steering column

Even though the occupant kinematics have been improved by the use of a knee airbag system, there is still an unfavourable upward movement of the steering column. The upward movement of the steering column leads to a severe contact of the lower steering wheel rim to the thorax, which results in a high chest deflection. To avoid this impact on the thorax, the steering wheel should remain in the original position or should even be pulled downward (“active steering column”, ASC).



Figure 11: Steering wheel position without and with ASC

With the help of the active steering column, the lining up of the steering wheel is particularly advantageous for the chest deflection value (see figure 12).

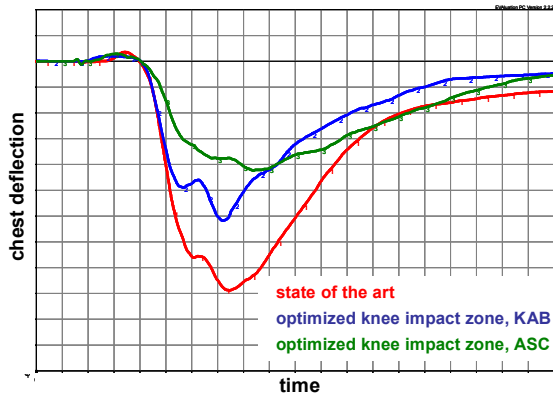
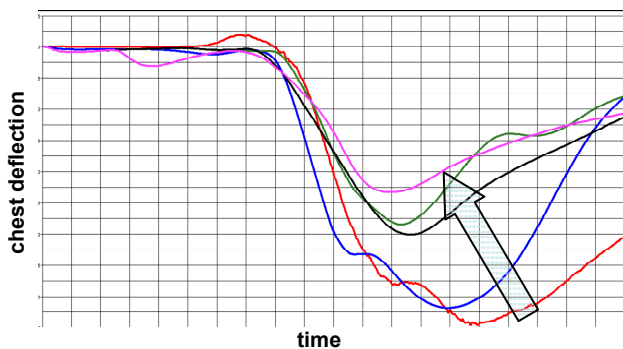


Figure 12: Impact of KAB and ASC on chest deflection

Restraint System Optimization

After conducting the sled tests, a CAE-model was validated and is ready to be used for further optimization steps for several restraint system components. By adjusting the vent hole diameter and the belt system (pre-tensioner, load limiter), a further improvement especially for the chest deflection under the “trailer back barrier”-load condition is possible.



- state of the art (test)
- state of the art (simu)
- optimized knee impact zone, KAB (simu)
- optimized knee impact zone, KAB, ASC (simu)
- optimized knee impact zone, KAB, ASC, RHS adjusted (simu)

Figure 13: Chest deflection

After optimizing the restraint system, the kinematics of the dummy and the way the driver airbag is working come much closer to the behaviour of a passenger car restraint system (see figure 14).



Figure 14: Improvement of dummy kinematics

Conclusion

The intrusion device was introduced as a new sled test method. With the help of this method it was possible to investigate new concepts for restraint systems for heavy trucks, because even the behaviour of the knee impact now correlates sufficiently to the full scale test. As new components for the Heavy Truck Restraint System a Dual Knee Airbag and the Active Steering Column were introduced. Together with the known components of a restraint system, these new components contribute to an optimized system, which shows a comparable performance to a passenger car system regarding kinematics and working principles.

References

- [1] R. Zinser, Ch. Hafner, Der LKW-Unfall aus unfallmedizinischer Sicht; VKU April 2006
- [2] <http://www.feuerwehr-ahrweiler.de>, 15.02.2011

OPTIMIZATION OF SEAT BELT BUCKLE MOTION FOR REDUCING CHEST DEFLECTION, USING RIB EYE SENSORS

Burkhard Eickhoff

Werner Schrenk

Harald Zellmer

Autoliv B.V. & Co. KG, Elmshorn, Germany

Martin Meywerk

Helmut-Schmidt University, Hamburg, Germany

Paper Number 11-0098

ABSTRACT

To achieve overall good ratings in frontal impacts according to US and Euro NCAP, low chest deflection values have to be obtained. Concerning belt induced chest deflection, belt forces as well as the geometry of the belt system have to be optimized. Hence, the objective of this study was to analyse the influence of the buckle position and motion during crash on chest deflection.

Theoretical investigations as well as simulations (software MADYMO / Facet - Q-dummy) were used to study the influence of the buckle position and motion on chest deflection. Sled tests, where the environment represents a middle class vehicle, were conducted to verify the findings. In order to obtain detailed insight regarding the deformation of the HIII 50% dummy's thorax and the load distribution, rib eye sensors were used showing the deformation of each individual rib during the crash.

As an outcome, the rib eye sensors show an unbalanced thorax deformation. Relevant differences in rib deformation are observed between left and right ribs of the thorax. Smaller differences are seen between upper and lower ribs. Concerning chest deflection, simulation and test results show an important influence of the buckle motion on chest deflection and on the energy absorption of the dummy. Significant differences in load distribution are detectable by the usage of rib eye sensors.

The retention of a Hybrid III 50% dummy with a 3-point belt leads to an unbalanced deformation of the thorax ribcage. To achieve low chest deflection values, the upper and lower diagonal belt force as well as the belt geometry have to be tuned. In fact, the belt geometry significantly influences the deflection of the ribcage. The buckle position and buckle motion during forward displacement of the dummy can be identified as significant tuning parameters.

1. INTRODUCTION

The risk of severe thorax injuries in frontal crashes is still relatively high compared to other body regions, cf. fig. 1. /1/. Chest deflection, measured with the HIII dummy has become more and more the important injury assessment value to evaluate the thorax injury risk in laboratory tests /2/. The rating of deflection instead of chest acceleration in the US NCAP frontal crash underlines this trend.

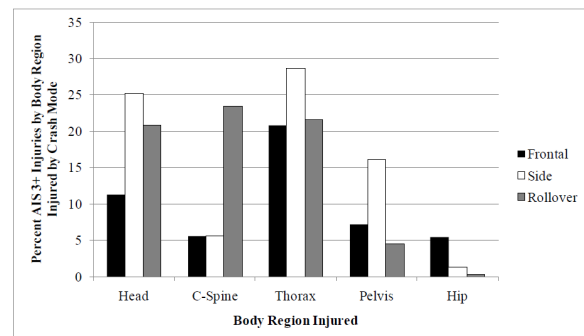


Figure 1. AIS3+ injury probability by body regions for frontal, side and rollover crashes in US /1/.

The measured chest deflection values of the Hybrid III dummy have to be interpreted with care. Due to a single measurement at the sternum with a slider, local penetrations of ribs cannot be identified. Furthermore, the deformation of the ribcage is different compared to the Human thorax /3/ /4/. As a result of these considerations, the deflection values should be interpreted under consideration of the loading conditions /5/.

In this paper, simulation and tests with rib eye sensors /6/ are used to describe belt induced thorax deformation. Furthermore, it is shown that a more

balanced deformation of the thorax can be achieved by modification of the buckle tongue position.

2. THE BELT LOAD ON THE HYBRID III THORAX IN FRONTAL CRASHES

The diagonal belt load on the thorax can be described as a function of the belt forces F_{B3} , F_{B4} (cf.

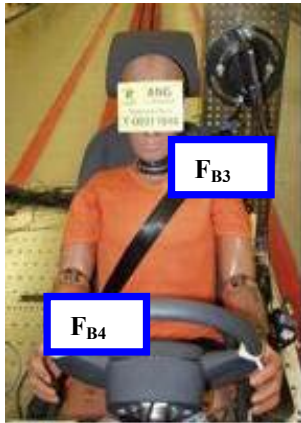
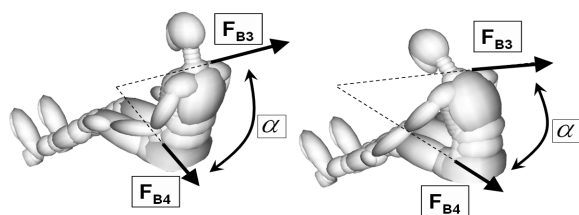


Figure 2. Location of belt force sensors.

fig. 2) and the geometry. Concerning the thorax deceleration, a simplified calculation of the resultant force can be used, cf. figure 3 /7/. As a result, the load on the thorax increases during the forward displacement of the dummy due to geometry effects.



$$F_{Res} = \sqrt{F_{B3}^2 + F_{B4}^2 - 2F_{B3}F_{B4} \cos(\pi - \alpha)}$$

Figure 3. Simplified computation of the resulting belt force on the occupant. Right: The forward displacement leads to higher forces acting on the dummy. Source: /7/

In contrast to this, belt induced chest deflections cannot be analysed with a simple calculation of the resultant belt force on the dummy. In fact, analysis about the loaded thorax regions of the dummy and the thorax deformation characteristic itself are necessary and -as a consequence- are part of the following investigation to evaluate favourable belt geometries.

3. METHODS

Theoretical considerations as well as simulation runs with MADYMO, sled-tests and static deployment tests were done in a generic environment. The used environment (fig. 4) can be described as the following:

- seat cushion on a rigid interface
- no airbag
- no instrument panel (no knee contact)
- belt system with load limiter and retractor pretensioning
- dummy Hybrid III 50th percentile with rib eye sensors
- pulse according ECE R-16



Figure 4. Generic environment, Hybrid III with rib eye sensors.

A rib eye sensors system was used as described in /6/. The sensors were mounted at a distance of +/- 9cm from the mid of the sternum, cf. figure 5. During testing, attention was paid to a correct belt fit and a constant dummy temperature.

Concerning simulation, the MADYMO Facet Q Dummy HIII 50% was used also supplemented with rib eye sensors at the same locations. To obtain most reasonable results, a belt fitting pre-simulation was conducted for each variation in order to achieve a correct belt fit on the dummy.

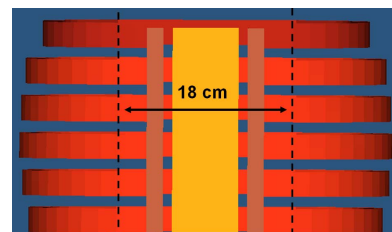


Figure 5. Locations of rib eye sensors.

4. SIMULATION AND TEST RESULTS

4.1 Actual thorax deformation and its measurement

To identify the difference between the slider measurement and the external deformation, static deployment tests were carried out. To eliminate the



Figure 6. Static deployment test with diagonal belt only and retractor pretensioning.

influence of the lap belt and abdomen, the dummy was loaded only by a diagonal belt with retractor pretensioning, cf. fig. 6. The result is given in fig. 7 where the webbing pay in and the chest deflection is plotted. As a result, the thorax deflection follows the webbing pull in with a delay reasoned by the viscoelastic deformation characteristic [8]. Furthermore, the difference between the web pay in and the deflection is not a result of the belt slack or

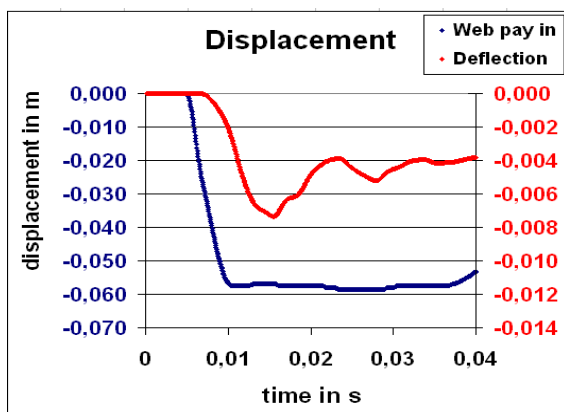


Figure 7. Web pay in by retractor pretensioning and chest deflection as a result.

belt elasticity only. In fact, a difference of the sternum deflection (measured with the slider) and external deformation can be noticed. As an example, a difference of about 10mm in the sternum area was

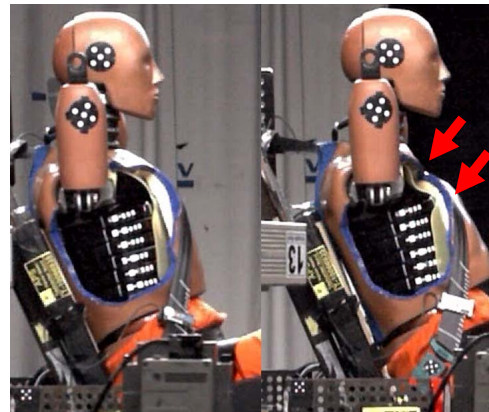


Figure 8. Foam deformation as a reason for different internal and external torso deformation.

found. To demonstrate the reason for this difference, tests with an open dummy jacket were carried out.

Figure 8 shows the deformation of the foam which can be identified as the main reason.

4.2 Thoracic response to belt loading in sled tests

During forward displacement of the Hybrid III dummy in frontal crashes, an unbalanced forward displacement can often be noticed, cf. fig. 9. The belt loaded shoulder shows more forward displacement than the unloaded shoulder, which seems to be unexpected. The reason for this behaviour can be



Figure 9. Higher forward displacement of the left shoulder even though it is loaded by the belt.

explained in figure 10. The dummy chest is loaded asymmetrically by the belt. In addition to the loading of the left shoulder and the sternum, in particular the right ribs are loaded by the belt, leading to unsymmetrical thorax retention.

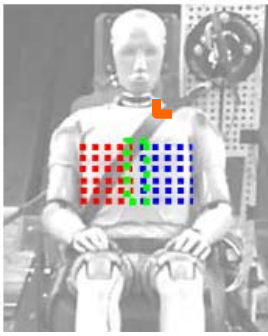


Figure 10. Belt load on the thorax: Mainly the right ribs and the left shoulder are loaded.

The unsymmetrical thorax deformation can be measured with the rib eye sensors in sled test, cf. figure 11. Main differences can be noticed between the left and right ribs. Furthermore, a difference between the upper and lower ribs can be found. While a decreasing in deflection of the unloaded left rib 1 to the left rib 6 can be measured, an increasing in deformation of the belt loaded ribs from the upper

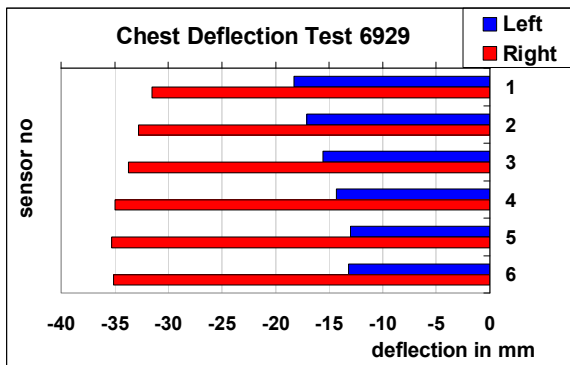


Figure 11. Ribs eye measurement results which show the unsymmetrical deformation.

ribs to the lower ones can be noticed. Figure 12 shows the simulation results. The difference between right and left ribs can also be shown. In contrast,

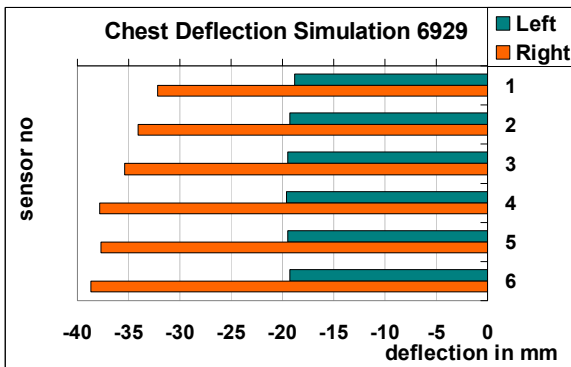


Figure 12. Simulation results of the rib deformation.

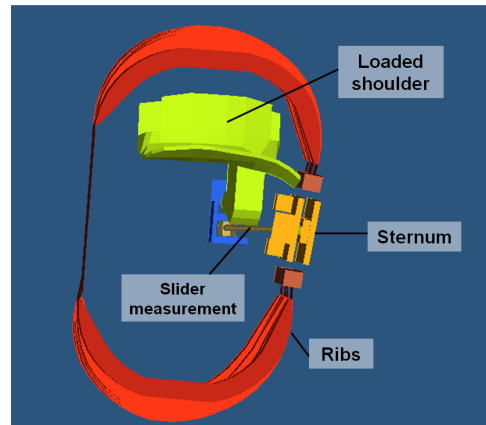


Figure 13. Loaded dummy ribcage in simulation.

differences between the 6 left ribs were not detected. In fig.13 the deformations of the ribs are visualized.

4.3 Modification of the buckle tongue position during crash

To investigate the influence of buckle tongue position during crash, sled tests were carried out. The variation parameter in these tests was different buckle motion during testing. Figure 14 shows the

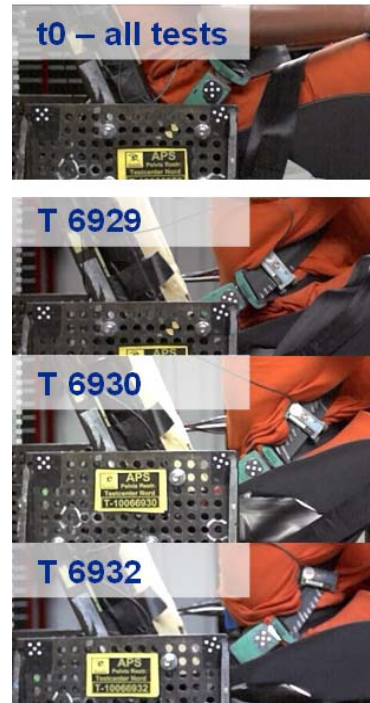


Figure 14. Different buckle motion during testing. Initial buckle position and the position at maximum dummy forward displacement is shown.

differences in three tests as an example. The initial buckle position at t_0 is identical; at maximal forward displacement of the dummy differences are evident.

As a result, relevant differences in chest deflection and load distribution are noticeable. In test 6929 the highest deflection values were measured. In test 6930 the differences between the loaded right and the unloaded left ribs decrease. Furthermore, the comparison between the loaded right ribs shows in test 6930 no increase in deflection from the upper to the lower ribs. An emphasis of this trend is given by the results of test 6931. It has to be mentioned, that the forward displacement of the dummy thorax was about 35 mm higher in test 6930 compared to test

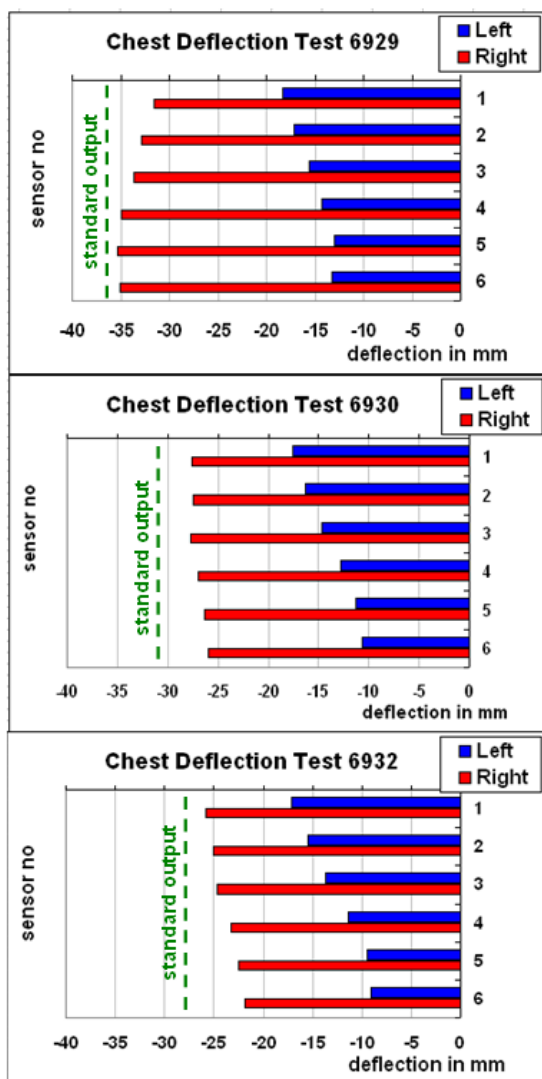


Figure 15. Influence of different buckle motion on rib deformation. Maximum value of each rib. Dotted line: dummy standard output (measured with slider)

6929. Test 6932 shows an increase in thorax forward displacement of about 51mm compared to test 6929. For all tests, the shoulder belt force F_{B3} was about 4.3kN, the belt force inner F_{B4} was measured in the range of 3.5kN to 4kN at the maximum chest deflection.

The simulation results of the tested configurations 6930 and 6932 also show a reduction of deflection values. On the other hand, the influence on the differences between the loaded upper and lower right ribs were smaller than in tests.

To compare the test configuration 6929 with 6930 correctly, the belt force on the shoulder was increased in simulation with configuration 6930 to

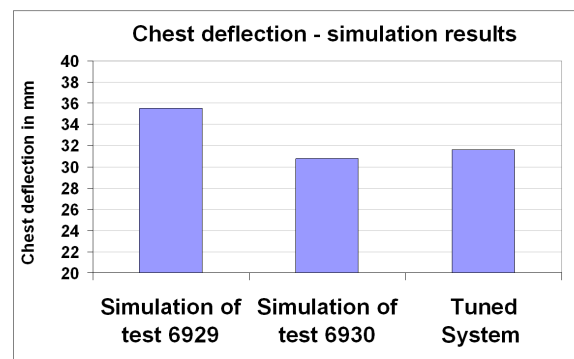


Figure 16. Simulation results of the maximal deflection (standard measurement). A benefit of about 4mm in chest deflection can be achieved with comparable dummy forward displacement.

achieve the same forward displacement as in run 6929. As a result, the benefit in deflection decreases down to 4mm, cf. figure 16.

Closing, in the chosen positions of the rib eye sensors the maximum values of all ribs were comparable or lower compared to the slider measurements of the dummy in all tested configurations, cf. fig 15.

5. DISCUSSION

To evaluate and optimize the thorax deformation by the belt, several items have to be taken into account. First, the viscoelastic thorax deformation characteristic can be seen as expected during the static deployment test (fig. 7). In addition, the differences between external and internal dummy deformation can be noticed which are not the result of the sternum deflection measurement alone. In fact, the foam of the jacket has a relevant influence on the external deformation, as demonstrated in figure 8.

Furthermore, the thorax is loaded by the belt mainly on the shoulder, the sternum and on one side

of the ribs, due to dummy design (fig. 10). This loading condition leads to an unsymmetrical thorax deflection (fig. 11). A relevant difference between the loaded and unloaded rib side can be noticed, in this test series it was up to 22mm (fig. 11). As a result of this deformation, an unsymmetrical forward displacement of the thorax follows, which can be an indicator for the unequally distributed load on the thorax. (fig. 9).

The advanced simulation model with the Facet Q MADYMO HIII 50% dummy shows also the difference between the left and right ribs (fig. 12), however, the used simulation model is less sensitive to altered belt geometries than the hardware dummy. This is true especially for the less loaded side of the ribcage. As the general behaviour of individual rib deflection is also seen in the simulation model, it is justified to using it for principle simulation runs.

To achieve a more uniform chest deformation, the belt geometry should be analysed and -if possible- optimized, in addition to the control over the shoulder belt forces F_{B3} and F_{B4} , cf. /9/. In this test series the buckle movement was modified as shown in figure 14 to point out the influence of the belt geometry on the deformation. Of course, the belt forces are influenced by the different buckle motion. In this test series the differences in belt forces at the maximum chest deflection are too small to be the reason for the different deflection values, if usual errors are assumed. In fact, the chest deflection is mainly influenced by the buckle tongue movement, which results in different belt geometries. A high influence of the tongue motion can be expected, especially by an unsymmetrical loading of the belt loaded ribs, cf. fig. 15.

During an optimization of the belt system concerning chest deflection, the forward displacement of the dummy has to be monitored to achieve comparable boundary conditions as done in simulation by increasing the shoulder belt load limiter. Furthermore, the coupling of the dummy, the pelvis retention (e.g. avoiding submarining) has to be taken into account. To achieve an optimum buckle movement, further investigations should be carried out in this direction.

Closing, this investigation was done in a generic environment without airbag and knee contact. Further investigations should be made to evaluate the benefit of an optimized buckle position and buckle motion in different vehicle environments with airbag and knee contact to the instrument panel. Furthermore, a variation of the rib eye sensor positions could give more information about the thorax deformation and answer the question whether such positions lead to measure the maximum deflection values of the ribs.

6. CONCLUSIONS

During the retention of a dummy in a frontal crash with a 3 point belt, the thorax deforms in an unsymmetrical manner. The reason for this is the unequal loading of the dummy. The belt loads one shoulder, a part of the dummy sternum and one side of the ribcage.

In the environment investigated, the used rib eye sensors show the expected different rib deformations. On the one hand, high differences between left and right ribs can be noticed. On the other hand, differences in deformation between upper and lower ribs can be measured. The latter indicates an unbalanced tuning of the belt system. Furthermore, the relevance of the lower diagonal belt concerning chest deflection can be noticed.

With the used simulation model, the principle rib thorax deformation can be calculated; however, the model shows less sensitivity to altered thorax loading than the hardware dummy.

To reduce the thorax deformation, the belt forces F_{B3} and F_{B4} as well as the belt geometry -which changes during dummy forward displacement- have to be optimized. Concerning that the webbing is re-routed in the buckle tongue, an improved buckle motion seems to be beneficial. In this investigation, a reduction in chest deflection of about 4mm could be achieved.

7. REFERENCES

- /1/ Ridella, S.A.; Scabro, J.M.; Rupp, J.D.; Schneider, L.W.: Improving Injury Causation Analysis and Coding in CIREN Using the BioTab Method. Proceedings of the 4th International ESAR Conference. Hanover, 2010
- /2/ Kent, R.; Patrie, J.; Benson, N.: The Hybrid III dummy as a discriminator of injurious and non-injurious restraint loading. AAAM, Annual Proceedings - Association for the Advancement of Automotive Medicine, 47; (2003)
- /3/ Kent, R.; Shaw, G.; Lessley, D.; Crandall, J.; Kallieris, D.; Svensson, M.: Comparison of belted Hybrid III, THOR, and cadaver thoracic responses in oblique frontal and full frontal sled tests. SAE, Paper No.: 2003-01-60, 2003
- /4/ Yoganandan, N.; Skrade, D.; Pintar, F. A.; Reinartz, J.; Scances Jr, A.: Thoracic Deformation Contours in a Frontal Impact. Proceedings of 35th Stapp Car Crash Conference, San Diego, USA, 1991.

/5/ Kent, R., Patrie, J.; Benson, N.: The Hybrid III dummy as a discriminator of injurious and non injurious restraint loading. Annual Conference of the Association for the Advanced of Automotive Medicine, Des Plaines, IL, 2003

/6/ Yoganandan, N.; Pitar, F. A.; Rinaldi, J.: Evaluation of the Ribeye Deflection Measurement System in the 50th Percentile Hybrid III Dummy. NHTSA final report 811102 , 2009.

/7/ Eickhoff, B.; Zellmer, H.; Meywerk, M.: The Influence of the Safety Belt on the Decisive Injury Assessment Values in the New US NCAP. Proceedings of the 2010 IRCOBI Conference, Hannover, September 2010.

/8/ Kent, R. W.; Crandall, J. R.; Rudd, W.; Lessley, D.: Load Distribution-Specific Viscoelastic Characterization of the Hybrid III Chest. Paper SAE 2002-01-0024, 2002

/9/ Eickhoff, B.; Zellmer, H.; Forster, E.: The mechanism of belt induced chest deflection: Analysis and possibilities for reduction. Proceedings of 20th ESV Conference, Lyon, 2007

STUDY ON STEERING COLUMN COLLAPSE ANALYSIS USING DETAILED FE MODEL

Tae Hee, Lee
Byung Ryul, Ham
Seong Oh, Hong

Advanced Safety CAE Team / Hyundai Motor Co.
Korea
Paper No. 11-0262

ABSTRACT

EASC(Energy Absorbing Steering Column) is a kind of Steering Column which minimizes the injury of the driver during a car accident by collapse or breaking particular part of system. Up to now, Steering Column in Crash Analysis had no way to describe these 'Collapse' or 'Slip' by the Axial and Lateral Forces from driver. In this paper, we have created a new Steering Column using a Detailed FE Model which can describe such collapse behavior.

INTRODUCTION

EASC (Energy Absorbing Steering Column) is a type of Steering Column which minimizes the injury of the driver during a car accident by collapse or breaking particular part of system. Up to now, it has been difficult to assess the Collapse behavior and energy absorption of the Steering column in frontal impact analysis because of the rigid body FE joints of column model. Also, in cases of occupant analysis model, the loading characteristics of the column are described using a F-D Curve from the static axial compression test, but the reliability of the load in the arbitrary direction is low except for the load in the axial direction.

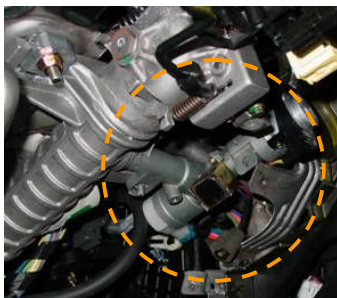


Fig.1 Key Set-Knee Bolster MT'G interference

Therefore, in case of Steering Column Collapse, it's impossible to check interference of the surrounding parts (Fig.1). It is also impossible to predict or respond

to Collapse test distribution (Fig.2).

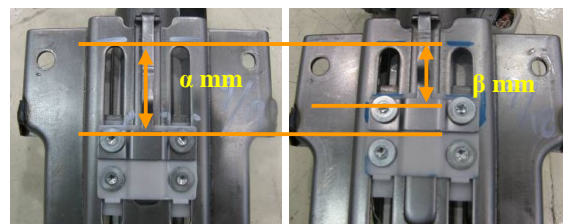


Fig.2 Column Collapse distribution of sled test

Thus we need to develop an analysis model that can describe the collapse behavior of the steering column under the arbitrary loading condition.

Accordingly, in this study, we have developed a detailed FE model that can describe the collapse behavior to cope with FE-Occupant Full vehicle analysis and FE-Multi body coupling analysis that will progress from hereafter.

The condition for the Steering Column analysis model developed in this study is as follows

- It should be able to describe the Collapse movement of load in the arbitrary direction.
- It should be able to describe the static compression test result.
- It should be adaptable to the Full car frontal impact analysis (US NCAP full frontal, EuroNCAP offset etc.).

In this study, we have selected 4 types of representative Steering Column (type A, B, C, D) to develop an FE model that satisfies the above terms. Using this, we established a Steering column analysis method through the following procedures.

- 1) Steering column static compression test correlation
 - Build capsule pin fracture model and correlation.
 - Build curling plate model and component correlation.
 - Fastening load and friction component correlation
- 2) FMVSS203 Body Block Test Correlation.
- 3) Verification of detailed column model using Madymo Input and Sub-Structure analysis.

All analysis was progressed using LS-Dyna Version 971 Revision 4.

BUILD DETAILED FE MODEL AND STATIC COMPRESSION TEST CORRELATION

The steering column developed through this study was made to apply to FE-Occupant Full vehicle analysis and FE-Multi body coupling analysis. For this, it should show a practical behavior in arbitrary loading condition that can be delivered through a test dummy. Therefore, in composing a model, we focused on the following concept and tried to exclude any non-practical collapse behavior.

- 1) Avoid rigid body modeling: Actual joint modeling for kinematical locking.
- 2) Friction and deformation from contact forces.
- 3) Following actual geometry and tolerance.

After analyzing the 4 selected steering columns, we could confirm 4 factors that had direct influence on collapse load.

- Capsule Pin
 - Curling Plate
 - Friction force from fastening load of bolt
 - Friction Force from expending tube and collapse ring
- By analyzing the effect of such factors, we could progress static compression test correlation in each steering columns.

Capsule pin fracture model correlation

Capsule pin is a plastic injection pin connecting the Al capsule and column which was usually ignored in traditional analysis models. In this study, we assumed the Capsule Pin as a cubic element with 1mm height (Fig.3). Tied Contact method was used to bond to the basic material, and Stress Based Failure criteria was used to model the fracture of Pin through shear force. (Fig.4)

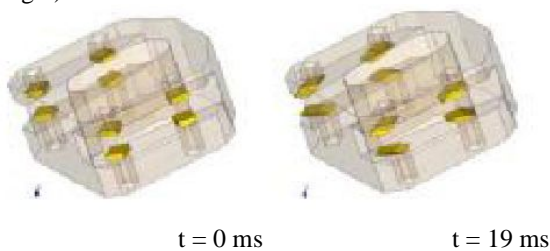


Fig.3 Capsule Pin modeling and Static Test

Using this Capsule Pin model, we conducted a Correlation about Capsule Pin component static test. Correlation was progressed by adjusting the following factors.

- Young's Modulus
- Hardening Modulus
- Failure Effective Strain
- Failure Shear Stress
- Rupture Strain

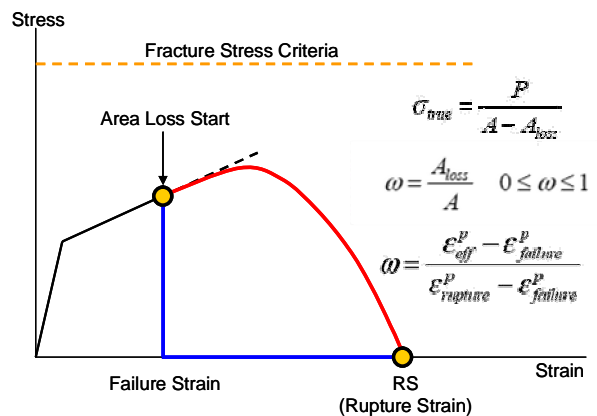


Fig.4 Fracture Stress Criteria

Fig.5 is the graph showing the result of the Static Test Simulation. We can see that the completed model has the characteristics of the actual Capsule Pin.

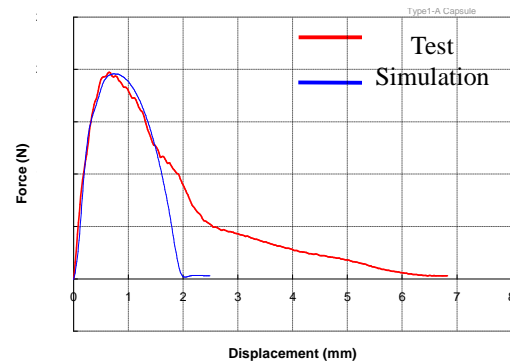


Fig.5 Capsule pin static test vs. Simulation

Curling Plate correlation

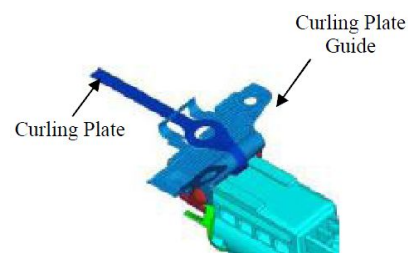


Fig.6 Modeling of Curling Plate

Curling plate is a component that controls collapse load of steering column. It is used to attain target collapse load through adjusting the thickness, width, and form. Change of collapse load by the design of curling plate is digressing from the main subject of this study, and therefore will not be handled. In this study, we tried to describe the given shape of the Curling Plate as detailed as possible, and conducted correlation with component test. (Fig.6) Fully Integrated Shell element

was used for FE model and integration point was set to 5 point at thickness direction to obtain bending stiffness. 1.5mm element was used to describe the Curling Plate and bending part of Guide. True Thickness Contact was used in every Contact related to Collapse, and to exclude the effect of friction between Curling Plate Guide and Column, the coefficient of friction was set at 0.0.(Fig.7)

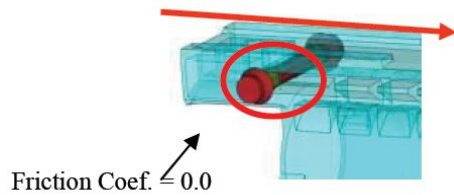


Fig.7 Modeling of Curling Plate

Fig. 8 is a graph showing the result of Curling Plate F-D test Simulation. It can be observed that the completed model is following actual characteristics.

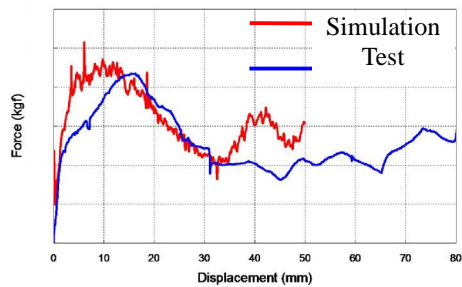


Fig.8 Curling Plate Correlation F-D Curve

Fastening load correlation

Fastening load is a friction load generated from fastening component, such as Bolt and Pin. In column FE model, fastening load of curling plate guide fastening bolt and tilt lever fastening bolt should be considered. If fastening load exists, normal force which is stronger than that of usual contact from geometry occur. Therefore, when realizing a collapse behavior according to friction and deformation, fastening load must be considered. In this study, Steering Column of A and C are relevant.

Friction from fastening load can be calculated by the following method.

- 1) Calculate the axial force of bolt from designed bolt torque.
- 2) Calculate the stress of bolt section.
- 3) Apply the calculated stress to the bolt section, using 'Initial Stress Section Card.
- 4) Check the stress contour during correlation analysis (Fig. 10)

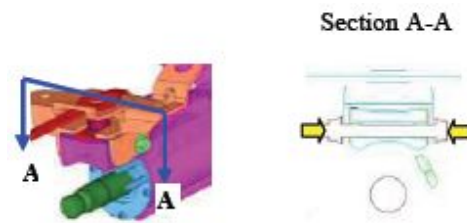


Fig.9 Normal force from fastening bolt

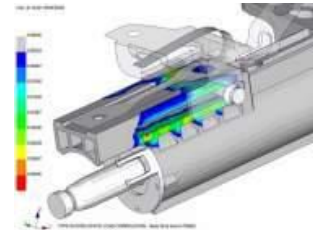


Fig.10 Stress contour from fastening load

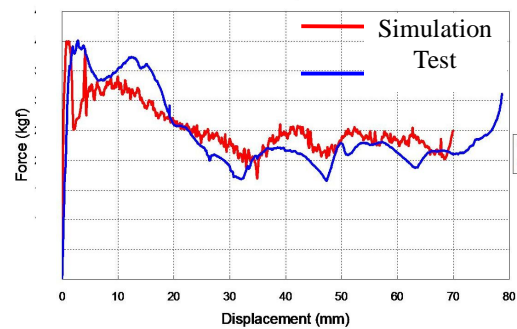


Fig. 11 Static compression test correlation of steering column type A

Fig.11 is a graph showing the result of static compression test of Steering Column type A. We can see that the completed model has the actual characteristics.

Of the 4 factors mentioned above, the ones that affected the Steering Column type A are the following three.

- Capsule Pin
- Curling Plate
- Friction force from fastening load of bolt

Friction component load correlation

Friction component load is the friction force that rises from collapse ring used in steering columns of expended tube type. Collapse Ring is a friction component that exists between the steering column housing and the main tube of the column. (Fig. 12)

In this study, the steering column of type B and D uses these friction components. Correlation was conducted under the assumption that all friction force of steering

column rises from the collapse ring.

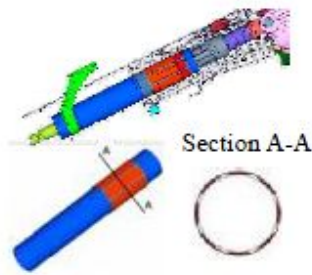


Fig. 12 Collapse Ring Modeling

Collapse ring uses rigid material. After analyzing the result of the static compression test results of column type B and D, we set the friction component load on α - β kgf to conduct the correlation.

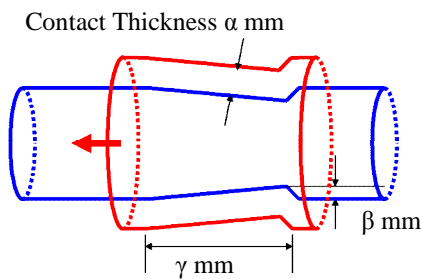


Fig. 13 Collapse Ring Modeling Concept

Fig.13 is the schematic diagram representing the modeling of friction component. As shown in the picture, the collapse ring (red line) and column tube (blue line) have a minute slant and step. This slant and step lead the tube's deformation when collapse progresses in the direction of the red arrow.

In order to compensate for the deformation at the initial state, we conducted a pre-analysis of moving the collapse ring forward from δ mm behind the original location. The stress of the tube can be adjusted by pre-stress condition using INITIAL STRESS SHELL card and you can attain the target friction force. (Fig. 14, 15)

Fig.16 is a graph that shows the simulation results from the static compression test of the steering column type B. We can see that the simulated results well follows the real characteristics.

Of the 4 factors mentioned above, the ones that affected the Steering Column type B are the following two

- Capsule Pin
- Friction Force from expending tube and collapse ring

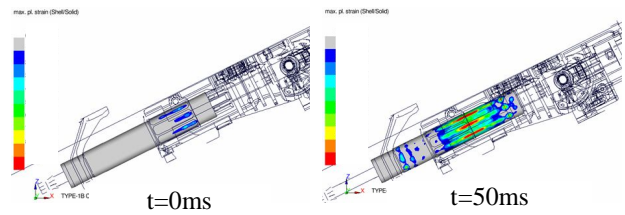


Fig. 14 Stress contour of column (before/after)

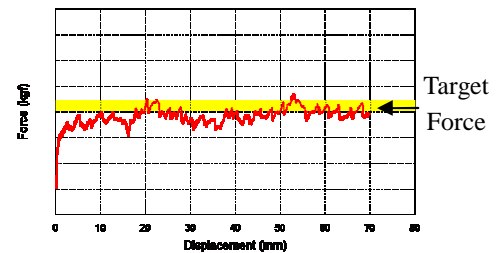


Fig. 15 Friction force F-D curve of steering column type B

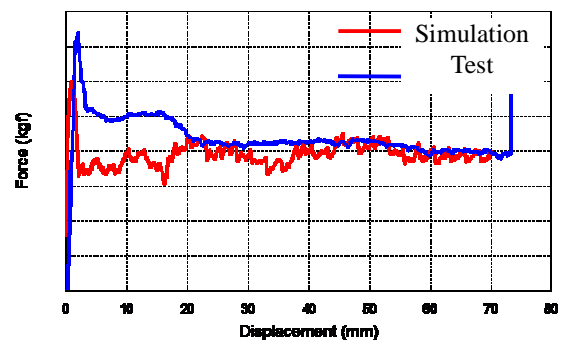


Fig. 16 Static compression test correlation of steering column type B

FMVSS203 BODY BLOCK TEST CORRELATION

FMVSS203 is a Steering Control System related regulation. The purpose of FMVSS203 is to minimize chest, neck, and facial injury in case of frontal impact. In FMVSS 203 test, a body block of approximately 36kg directly collides into the steering column with initial velocity of 15 Mph(24Km/h), and the maximum load of body block and steering column should not exceed 2500 lbs (11kN). Fig.17 describes the schematic diagram of the body block test.

In this study, body block test correlation is conducted with each 4 type of steering column and intermediate shaft.

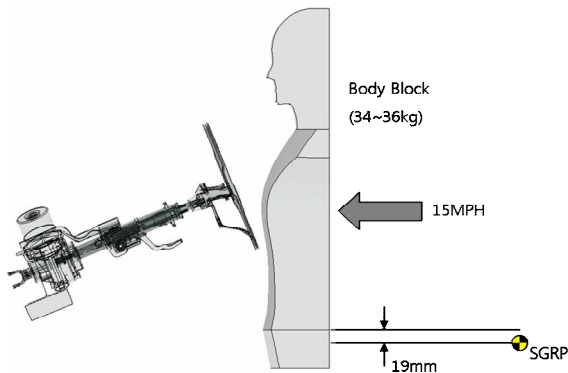
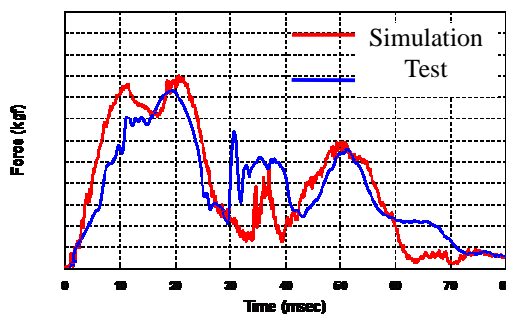
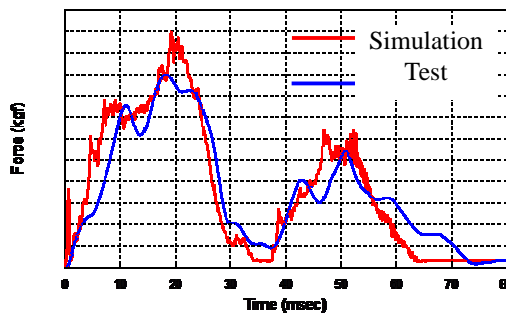


Fig. 17 Body Block Test



Load Cell Force



Body Force

Fig. 18 Type D Body Block Test Correlation

Fig.18 is a graph that shows the simulation results from the steering column body block test of column type D. It can be noted that static compression correlation models agrees with the actual characteristics of body block test

VERIFICATION OF DETAILED COLUMN MODEL USING SUB-STRUCTURE ANALYSIS

Final goal of this study is the development of steering column system which is available for FE-Occupant Full vehicle analysis and FE-Multi body coupling analysis. To do this, steering column model should have the following characteristics.

- 1) Description of the collapse behavior according to the

load applied in arbitrary direction.

2) No Time Step and Mess Scaling problems.

3) Rapid response for modifications of restraint system.

In order to satisfy 2) and 3), our study reviewed the possibility of steering column using sub-structure analysis rather than through full vehicle analysis.

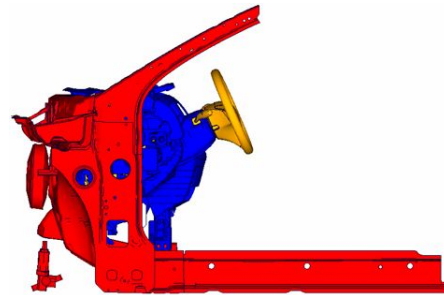


Fig. 19 Boundary condition of Sub-Structure analysis

Fig.19 represents boundary conditions of sub-structure analysis developed in our study. Procedural steps are as follows.

1) Extract sub-structure boundary condition data from the components which can influence column collapse behavior in US NCAP frontal analysis. (Fig.17 Red components)

2) Build sub-structure analysis model including crush pad, detailed steering column system, etc.

3) Input the x/y/z direction load extracted from occupant analysis (using MADYMO) as a curve according to time.

4) Run the sub-structure analysis and verify the collapse behavior of detailed steering column system.

Since our FE-Occupant Full vehicle analysis is not yet established, for the collapse behavior, we input the x/y/z direction load extracted from occupant analysis (using MADYMO) as a curve according to time.

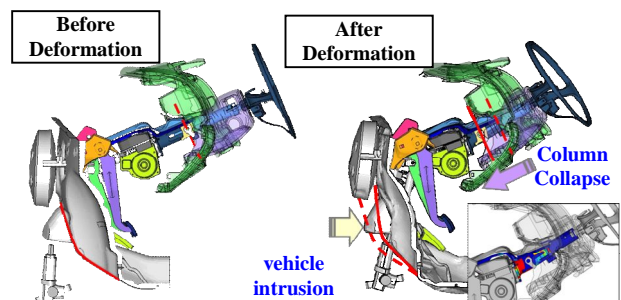


Fig. 20 Sub-Structure analysis result (Side View)

Fig.18, Fig.19 is the result of US NCAP frontal analysis using sub-structure analysis proposed by our study. A detailed model (type C) collapsible to load in the arbitrary direction that was developed by this study was used, and body and other data were extracted from the full vehicle model. The collapse behavior was well

described and interference between column and pedal mounting during collapse behavior was also well described. Therefore, the detailed column system is expected to be readily applied to the FE-Occupant full vehicle analysis.

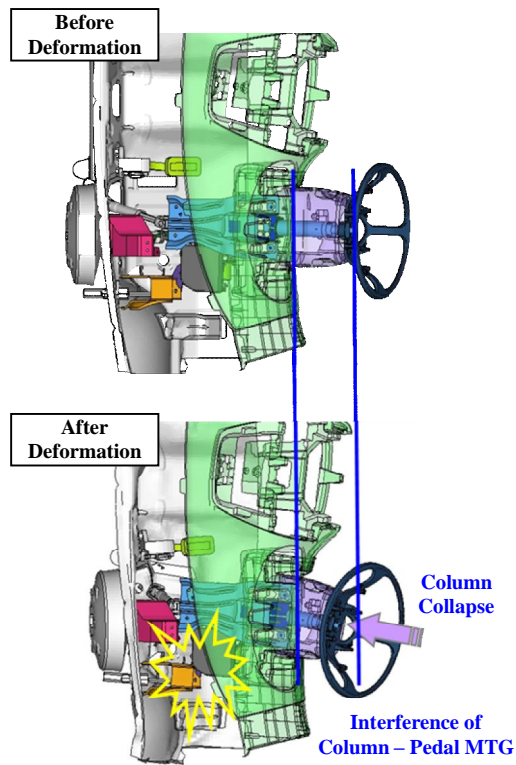


Fig. 21 Sub-Structure analysis result (Top View)

CONCLUSIONS

In our study, we developed a detailed model of a steering column that can be applied to the FE-Occupant full vehicle analysis. And using this, established a steering column collapse analysis method. The detailed model and analysis method developed in this study have the following characteristics:

Detailed modeling

- Deformable materials were used in defining most parts to consider the effects that can be caused from column bending and etc.
- Unusual behavior that can occur from rigid component was minimized by describing every mechanism in actual shape and not using rigid FE joint, except for on some bearings.
- Friction component and collapse load component, such as curling plate and collapse ring, contact thickness is defined as actual thickness, and by removing initial penetration, the contact was precisely

described.

- The collapse ring that is hard to describe as its original shape was realized through a simplified FE model that reflects the same concept.

Correlation

- By simplified model of the capsule pin, we developed a material that reflects failure properties of capsule pin.
- Correlation was performed by defining the initial stress at the parts where pre-stress exists by fastening load.
- When using the curling plate as the main collapse control part, we can identify the degree of contribution of the curling plate.

Sub Structure Analysis

- Substructure modeling methods that shows same behavior with full vehicle analysis was developed by inputting the crash results.
- The effects of the dummy, airbag and other restraint system could be evaluated by the results of occupant analysis.

The expected effect from proposed analysis method is as follows:

REFERENCES

- [1] NHTSA, "Laboratory Test Procedure For FMVSS 203 - Impact Protection for the Driver from the Steering Control System", 1990.
- [2] LSTC, "LS-Dyna Keyword User's Manual Version 971", 2007